Correlation between macroscopic sugar transfer and nanoscale interactions in cation exchange membranes

Alessio Fuoco [a,b,c,d], Sylvain Galier [a,b], Hélène Roux-de Balmann [a,b,*], Giorgio De Luca [c]

[a] Université de Toulouse, INPT, UPS, Laboratoire de Génie Chimique, F-31062 Toulouse cedex 09, France
[b] CNRS, Laboratoire de Génie Chimique, F-31062 Toulouse cedex 09, France
[c] Research Institute on Membrane Technology (ITM-CNR), University of Calabria, Via P. Bucci, I-87036 Arcavacata di Rende (CS), Italy
[d] Department of Environmental Engineering and Land and Chemical Engineering, University of Calabria Via P. Bucci, cubo 44A, 87036 Rende (CS), Italy

A B S T R A C T

Previous experimental work has shown that the transfer of organic solutes through ion-exchange membranes depends on the membrane counter-ion and that this dependence is probably linked to the interactions taking place at the nanoscale inside the membrane matrix. In this paper, a computational approach is carried out, combining quantum mechanics and molecular mechanics to determine the in-teractions occurring at the nanoscale, taking a cation exchange membrane as example. Building blocks are first accurately studied at high level of quantum theory, before being merged in macromolecular models. The computed interactions are then compared to the experimental values of the solute flux in order to point out the nanoscale mechanisms governing the solute transfer. The computed gluco-se−polymer fragment interactions, related to the sugar solubility inside the membrane, are found to be almost independent from the membrane counter ion. On the contrary, significant variations of the chain−chain interaction, i.e. the interaction energies *per* trapped water molecule or hydrogen bonding wire connecting the polymer fragments, were observed according to the cation. Moreover, a correlation was pointed out with the experimental sugar fluxes obtained with 3 different sugars. Increasing chain−chain interactions inside the membrane was found to give decreasing sugar flux. Then this work shows that the cohesion energy between the polymer fragments fixes the dependence of the sugar flux versus the membrane counter-ion. The crucial role of the water molecules coordinating the cations is also highlighted.

1. Introduction

In agreement with the Global Footprint Network, human demand exceeds the regenerative capacity of our natural ecosystem [1] thus process intensifications are highly required.

Process intensification is a concept introduced in the chemical industry in the beginning of our century to minimize the environmental impact, reducing energy and raw material consumption, increase the safety and reduce the plants size. Membrane processes meet these preliminary conditions due to their lower energy consumption (in comparison with traditional methods), their capability to transport in an efficient and selective way specific compounds (recycling of water, chemicals and/or raw material), their potential to boost the reaction processes and their peculiarity to be built in modules can decrease the plants size [2–4].

An example of process intensification by membrane processes is the desalination of water. The request of fresh water is increasing while its sources are decreasing, thus desalination systems are more and more growing [5]. In this context, membrane processes can play an important role. For example the energy required to desalinate seawater by evaporation is approximately 18–37 kW h m^{-3}, while the energy required using membrane technology is lesser than 4 kW h m^{-3}. This difference in energy consumption explains why, membrane technology is used to produce more than 50% of desalinated seawater [6,7].

In addition, many other applications can be addressed by membrane technology to improve the process performances such as: wine productions (cold stabilization), deacidifications of fruit juice, whey demineralization, treatment of brines, lixiviates, production of green chemicals building blocks (organic acids), purification of saccharides, textile industry waste treatment etc.

Nevertheless, the expansion of membrane processes still suffers from the fact that it is hardly possible to predict their performances when new applications or stronger constraints are

* Corresponding author at: CNRS, Laboratoire de Génie Chimique, F-31062 Toulouse cedex 09, France.
E-mail address: roux@chimie.ups-tlse.fr (H. Roux-de Balmann).

considered. In fact, these processes are very sensitive to the composition of the feed solutions and to the environmental conditions in general.

In the process intensification framework, Electrodialysis (ED), a mature membrane process, can take a significant place. ED is applied from more than 50 years in the brackish water desalination or in the desalination of sea water to produce drinking water. But in the last decades other membrane processes, like nanofiltration or reverse osmosis, became predominant in such applications. However, nowadays, electrodialysis is investigated and applied in a large number of projects dealing with process intensification in environmental, chemical, food and drugs industry [8].

Recent experimental studies have demonstrated that the ionic composition of the solution, i.e. the nature and concentration of the ions, has a significant impact on the transport of neutral organic matter through ion exchange membranes like those used in electrodialysis [9]. Solvent (water) and organic matter (saccharides of different molecular weights) transfer were measured, in a diffusion regime, through a CMX cation exchange membrane (sulfonated polystyrene-divinylbenzene, Neosepta Tokuyama corp. Japan) soaked in different electrolyte solutions: NaCl, $CaCl_2$, $MgCl_2$ and NH_4Cl. It was found that the sugar fluxes are influenced by the membrane counter ion. For xylose, glucose and sucrose, decreasing flux was observed when the membrane is equilibrated with cations of increasing hydration. It was concluded that the solute transfer modification was mainly due to a modification of the membrane properties. But no variations of the membrane macroscopic characteristics were observed indicating that membrane modifications at the nanoscale are involved. The understanding of the mechanisms, at the molecular level, and interactions governing such trends is thus crucial to optimize the Electrodialysis process.

Thus, in this work, the correlation between nanoscale interactions occurring in a CMX membrane on one hand and the sugar transfer on the other hand is investigated by means of a combined molecular modeling free from adjustable parameters. Previous ab-initio (quantum) studies have highlighted the crucial role of noncovalent interactions, and in particular hydrogen bonding, on the polymeric membrane properties, such as the ion exchange capacity, molecular affinity and the non-linear increase of the water sorption as function of additive content in polymer [10–13]. In particular, the present work is focused on the noncovalent interactions and molecular mechanism by which the counter-ions, used to soak a cation-exchange membrane, affect the fluxes of sugars. Building blocks, such as the hydrated polystyrene monomers neutralized with the different cations, Na^+, Mg^{2+} and Ca^{2+}, and the hydrated glucose were assembled in supramolecular structures i.e.: glucose – polymer complexes and double polymer chain fragments, representing different parts of the macroscopic system. Hence, these building blocks were first studied with a high level of quantum theory, before being assembled in supramolecular models. In their turn, these larger models were studied by means of a Quantum and Molecular Mechanics approaches (QM/MM). Then polymer – sugar interactions as well as chain – - chain interactions are computed and compared to the sugar flux obtained experimentally.

2. Computational approaches

An accurate assessment of noncovalent interactions requires quantum chemical approaches; however, quantum calculations need also long computational times. When noncovalent interactions at the nanoscale have to be investigated in large systems, as in this work, Quantum Mechanics and Molecular Mechanics (QM/MM) approaches have to be applied. QM/MM methods have proven to be reliable and helpful in investigating such large systems [14–16]. Thus, here, building blocks were first studied at quantum level and then for larger systems (more than 100–150 atoms) a QM/MM method was adopted.

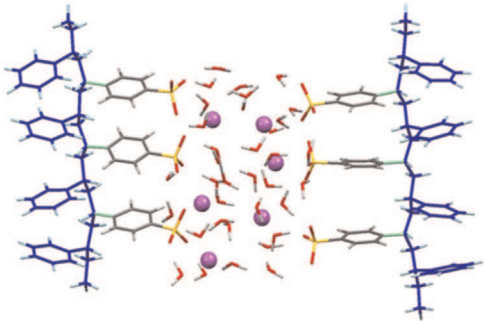

Fig. 1. Model used in QM/MM calculations. MM region in blue color, boundary in green color, other colors indicating the QM region. (For interpretation of the references to color in this figure legend, the reader is referred to the web version of this article.)

In the QM/MM approaches, a large system is divided in two regions: a classical part (less computational expensive) treated at MM level and a quantum zone. In general, the non-interacting atoms of the macromolecular system define the classical region, whereas the atoms involved in short range interactions, such as hydrogen bonds and electrostatic interactions, delineate the quantum region. In Fig 1, an example of quantum and classical regions are shown.

The total energy of the large model (Fig. 1) is calculated as the sum of the energies of classical and quantum parts. As regards, instead, the geometries optimizations carried out by the used QM/MM method, a step by step energy minimization of the two separated regions is carried out. In the first step, the QM region is optimized fixing the MM atoms. Afterwards a MM step is run for the optimization of the classical region with QM atoms characterized by a quantum potential; the cycle is repeated until the convergence criteria are reached.

A conformational research of the sulfonated styrene fragments was also carried out in this work. This task was performed at Molecular Mechanics level by using the Avogadro code [17] and the Universal Force Field [18]. A weighted rotor search of the more probable conformers and subsequently MM optimizations (500 steps and convergence energy criterion at 10^{-8} a.u.) was carried out. The energy of each conformer was then calculated at quantum mechanics level to select the most stable among them.

Both pure QM and QM/MM calculations were performed using NWChem 6.1 [19,20] code in the frame of Density Functional Theory and using the X3LYP [21] hybrid functional due to its reliability in the modeling of noncovalent interactions in polymer-solute – water systems [10-12]. Basis sets and convergence criteria were set depending on the size of the quantum models or quantum parts in the investigated macromolecules such as the hydrated counter-ions, glucose and large models as shown in Fig. 1.

The hydration of counter-ions attached to the sulfonated monomers was computed by adding water molecules to cations one by one and then optimizing at QM level the structures of the complexes, obtained after each H_2O insertion. The QM optimizations allow the relaxation of the entire water cluster around each cation finding new water arrangements at each insertion steps. The criteria, used for the QM geometry optimizations, were the maximum and root-mean-square of total energy gradients equal to 4.5×10^{-4} and 3.0×10^{-4} a.u., respectively, and the maximum and root-mean-square of the Cartesian displacement vectors equal to 1.8×10^{-3} and 1.2×10^{-3} a.u, respectively. The energy convergence threshold for the quantum self-consistent field

procedure was set to 10^{-6} a.u. and the root-mean-square of the electron density was set to 10^{-5} a.u. Basis sets for these calculations were 6−31 G* for C, H, S, O and 6-31++G for Na^+, Mg^{2+} and Ca^{2+}.

As regards the QM calculations of hydrated glucose in vacuum, energy and geometry optimization convergence criteria were set as outlined above, while the 6–31 G* basis set was used for all the atoms. The procedure used to evaluate the glucose hydration was similar to that used to get the hydration of counter-ions by using as starting geometry the glucose $(H_2O)_6$, since 6 water molecules interact with all the −OH groups and the ether oxygen of sugar.

Both counter-ion and sugar hydration shells were achieved when the interaction energy between the glucose or cations and the water molecules reaches a plateau. The Basis Set Superposition Error (BSSE) correction [22] was applied to obtain the energies associated to the interactions between monomer−cation complex and water, as well as the glucose and H_2O cluster.

To describe the MM regions in the QM/MM calculations, a Force Field has to be defined. Thus, the reliability of two Force Fields, Amber [23] and Charmm [24], with respect to the studied systems was investigated. The updated Charmm parameters for the cations, defined by Beglov and Roux [25], were used. In particular, some polymer fragment-cations were first optimized at DFT level and then by using DFT/Charmm and DFT/Amber approaches. The interactions between polymer fragment and cations and structural parameters obtained with the 2 force fields were then compared with the pure QM calculations. Concerning the geometrical properties of the neutralized polymer fragments both DFT/Charmm and DFT/Amber show a good reliability. As regards, instead, the interaction energies between the polymer models and cations, DFT/Charmm approach gives always results closer to the pure DFT values compared to the DFT/Amber method. Since the noncovalent interaction energies are the focus of this work, the DFT/Charmm method was preferred. A more detailed discussion on the Force Field assessment is reported elsewhere [26].

3. Results and discussion

3.1. Counter-ions and glucose hydration

The results, concerning the hydration of the cations in interaction with the polymer, are summarized in Fig. 2 and in Table 1. In particular, the number of water molecules added around each cation, attached to sulfonated monomers, until reaching the saturation limit is reported in the first column of Table 1. One can observe that the saturation limit depends on the kind of cation and it is respectively 10 water molecules for Na^+ and Ca^{2+} and 8 for Mg^{2+}. This difference is due to the more wedged position of the Mg^{2+} cation between the two SO_3^- groups compared to Na^+ or Ca^{2+}. The analysis of the optimized structures after each insertion of a water molecule reveals that they are arranged in two shells. In the first shell, the H_2O remains directly linked to the cation, as shown in Fig. 2 (spacefill atoms). Conversely, those comprised in the second shell, even if placed close to the cation in the starting geometries (i.e. before the QM optimization), move away from the cation, i.e. in a farther position (sticks in Fig. 2). In this position, they do not interact directly with the cation anymore since they are shielded by the ones belonging to the first shell.

Table 1
Number of water molecules added around each counter-ion, until saturation limit, and 1st hydration shell.

Number of H_2O molecules	*1st Shell Na^+*	*1st Shell Ca^{2+}*	*1st Shell Mg^{2+}*
1	*1*	*1*	*1*
2	*2*	*2*	*2*
3	*3*	*3*	*3*
4	*3*	*3*	*4*
5	*4*	*4*	*4*
6	*4*	*5*	*4*
7	*6*	*5*	*4*
8	*5*	*5*	*4*
9	*6*	*5*	*Nd*
10	*6*	*5*	*Nd*

Like the saturation limit, also the number of water molecules belonging to the first shell depends on the nature of cation, respectively 6 molecules for Na^+, 5 for Ca^{2+} and 4 for Mg^{2+}. Hence, the Ph-SO_3^--Na^+ $(H_2O)_6$, (Ph-SO_3^-)$_2$-Ca^{2+} $(H_2O)_5$ and (Ph-SO_3^-)$_2$-Mg^{2+} $(H_2O)_4$ systems were chosen as the starting geometries (i.e. the building blocks) for the building of the largest systems. The energies, associated to the interactions between the first hydration shell and the monomers-cation adducts, is high: -87.43 kcal/mol for Ph-SO_3^--Na^+ (H2O)$_6$, -146.78 kcal/mol and -157.44 kcal/mol for the (Ph-SO_3^-)$_2$-Ca^{2+} $(H_2O)_5$ and (Ph-SO_3^-)$_2$-Mg^{2+} $(H_2O)_4$ complexes, respectively. These values demonstrate that the complexes can be considered as stable substructures within the CMX polymer matrix. Conversely, since all the H_2O molecules belonging to the second hydration shell display lower energy of adhesion to the inner core, they were not included in the building block structures. Indeed, some of them can move or rearrange during the sugar diffusion in the matrix, as will be shown later.

The number of water molecules in the first hydration shell, obtained by the quantum optimized building block structures, can be compared with the experimental sugar fluxes. It should be remembered that the sugar fluxes in a CMX membrane equilibrated

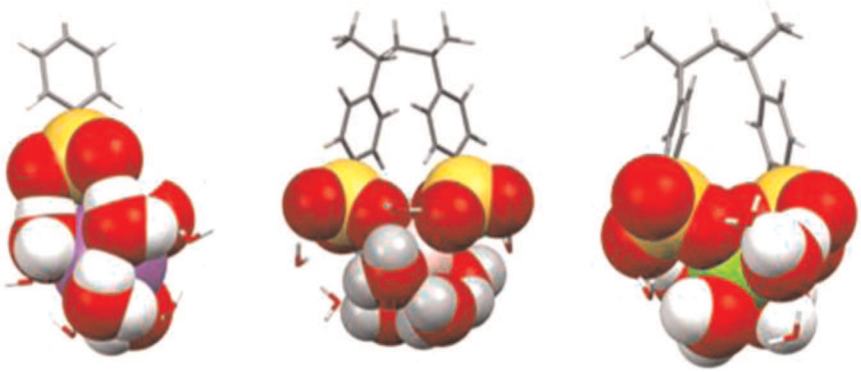

Fig. 2. Sulfonated styrene monomers neutralized by Na^+ (left, in violet), Ca^{2+} (middle, in pink) and Mg^{2+} (right, in green). Spacefill and stick atoms indicate the water molecules of the first and second hydration shell, respectively. (For interpretation of the references to color in this figure legend, the reader is referred to the web version of this article.)

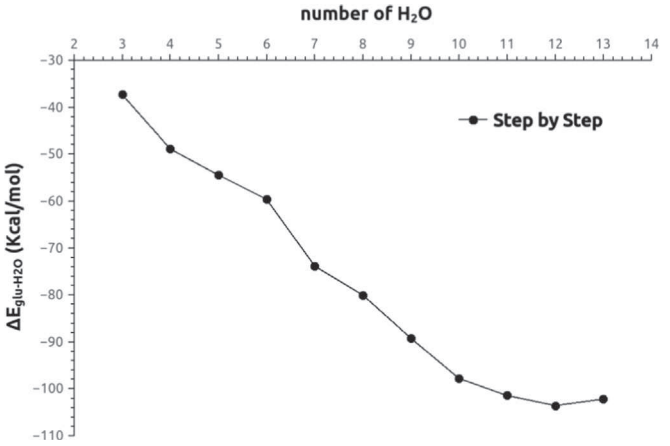

Fig. 3. Glucose – water interaction energy (in vacuum) as function of the number of water molecules (glucose hydration shell is built "step by step").

with Na^+ are higher than the ones obtained with the Ca^{2+} equilibrated membrane and that an even bigger difference was detected with Mg^{2+} used as counter-ion [9]. On the other hand, the optimized building blocks with Na^+, Ca^{2+} and Mg^{2+} reveal that 6, 5 and 4 water molecules are, respectively, involved in the first hydration cluster around the cation. Hence, the decrease of the sugar fluxes as function of the counter-ion can be related to the decrease of the number of H_2O molecules contained in the first coordination shell of the monomer.

As concerns the quantum calculations results of the interaction energy between glucose and the coordinating water clusters in vacuum, they are shown in Fig. 3.

Then, the glucose $(H_2O)_{11}$ is retained and chosen as the building block to model the hydrated sugar involved in the membrane – solute interaction. The interaction energy, corresponding to the plateau, is −101.5 kcal/mol, which roughly means an average energy of 9 kcal/mol for each single water molecule–glucose interaction. Considering that the energy of stable H-bonds are in the range of 10 kcal/mol [27], the hydrated sugar can be considered as another stable building block in the polymeric matrix as in the case of the neutralized sulfonated styrene monomers. Thus, the glucose $(H_2O)_{11}$ complex was used as the initial geometry to prepare larger models treated in successive QM/MM calculations.

An additional structure of a glucose molecule surrounded by 20 'randomly' arranged water molecules was also investigated to assess if the arrangement of the first hydration shell is influenced by the water molecules in the second shell. It was found that this hydrated structure, by only considering the first shell, is also less stable than the former glucose $(H_2O)_{11}$ selected complex.

A dimensional analysis of the sugar, at different hydration levels, was also carried out. The minimal molecular size, d_{min}, related to the smaller size needed for the transfer of the molecule in the membrane, and the effective diameter, d_{eff}, related to the average space needed for the transfer of the molecule were calculated for several glucose $(H_2O)_n$ structures using a home-made code described in previous works [28,29]. The effective diameter d_{eff} for each water – glucose system has been obtained by a home-made algorithm, on the basis of two specific dimensions: the height h and the rectangle enclosing the orthogonal projections of all atoms of the solvent molecule perpendicular to the principal molecular axis. The height h has been defined as the distance between the two most distant atoms of the water – glucose system taking into account their van der Waals radii. The minimum molecular size d_{min} has been obtained as the smallest size of the rectangle enclosing all orthogonal projections [29].

As was demonstrated in ref. [28], d_{min} is very similar to the molecular kinetic diameter. The values are reported in Table 2.

Table 2
Minimal molecular size, d_{min}, and effective diameter, d_{eff}, of glucose at various hydration levels in vacuum.

No H_2O – glucose	*d_{min} (Å)*	*d_{eff} (Å)*
6	*7.32*	*14.86*
7	*7.32*	*14.88*
8	*7.96*	*14.92*
11	*8.05*	*16.28*

One can state that both diameters have similar trends, i.e. increasing values for hydration level higher than 7 molecules. However, there is a great difference between the values of d_{min} and that of d_{eff}, whatever the hydration level. This is an important point to take into account since the sizes of the hydrated solute should be considered in the analysis of the correlations between sugar transfer and nanoscale interactions. However, the hydration shell of the transferring solute in the polymeric matrix can change with respect to that in the solution.

3.2. Key interactions: sugar – polymer or polymer – polymer

As previously explained, the influence of the membrane counter ion on the sugar flux was pointed during a former experimental work [9]. For each sugar, decreasing fluxes were observed when the membrane was equilibrated with cations of increasing hydration in solution, because in the polymer matrix the hydration of the cations is the inverse as it was outlined above. It was further concluded that nanoscale interactions taking place in the membrane were probably involved. Then, two kinds of interactions, i.e. polymer – sugar and chain – chain ones, were computed in order to determine which is the key interaction governing the dependence of the sugar flux with respect to the membrane counter ion.

3.2.1. Sugar – polymer interactions

The geometries of hydrated sugar – monomer structures were optimized at QM/MM level in order to assess the key noncovalent interactions at the nanoscale. In particular, the interactions between the sugar and the polymer were computed according to the previously described computational procedure, using the complexes shown in Figs. 5, 6 and 7, composed by the neutralized monomers, equilibrated with the cations, and the hydrated sugar. The contact spots between the hydrated glucose and the functionalized monomers were chosen minimizing the steric hindrance. Regarding the computational criteria, the only changes with respect to the thresholds used in the quantum optimizations of the single building blocks (i.e. neutralized monomers and hydrated sugar) concerned the maximum and root-mean-square of the Cartesian displacement vectors, here with thresholds of 5.4 and 3.6×10^{-3} a.u., respectively. The basis sets used were the 6 – 31 G* on the H, O, C, S atoms and 6 – 31 + + G on the cations. Concerning the classical region, the criteria were 10^{-4} nm for the threshold on the step size and 10^{-4} a.u for the total energy.

Different arrangements of the monomers around the hydrated sugar were taken into account. Both the hydrated glucose and the $(Ph\text{-}SO_3^-)_n$-cation define the QM region, while the other atoms of the complexes constitute the MM part.

The influence of the membrane counter-ion on the glucose transfer can have different origins. One can be the variation of the sugar solubility in the membrane, which is related to the interactions between the sugar and the polymer chains. Thus, the average energies, associated to the interactions between hydrated sugar and equilibrated monomers, were reported in Table 3 in addition to the interactions between glucose and its hydration

Table 3
Average energies, related to glucose – polymer fragments interactions ($\Delta E_{sugar-polymer}$). In the last column, the average energies associated to the glucose and its hydration shell interactions ($\Delta E_{sugar-water}$).

Counter-ions	$\Delta E_{sugar-polymer}$ *(kcal/mol)*	$\Delta E_{sugar-water}$ *(kcal/mol)*
Na^+	−78.01	−92.44
Ca^{2+}	−85.03	−88.06
Mg^{2+}	−85.15	−88.34

shell, $\Delta E_{sugar-water}$. These values are the average ones obtained considering the different arrangements of the monomers around the hydrated sugar, evaluated using the complexes shown in Figs. 5, 6 and 7.

The negative sign of $\Delta E_{sugar-polymer}$ and absolute values of these energies indicate that whatever the cation, the glucose is stabilized in the CMX matrix. The slightly higher energies associated with Ca^{2+} and Mg^{2+} complexes compared to Na^+ show that the sugar is more stable in the membrane matrix containing the divalent ions. But the values obtained for the different counter-ions are almost similar, in fact the difference not exceeding 7 kcal/mol.

One can then conclude that the interactions between glucose and the neutralized polymer fragments do not explain the observed counter-ion influence on the sugar fluxes. In fact, the sugar flux in the membrane equilibrated with Na^+ is more than 2 times higher with respect to that measured [9] with the same membrane equilibrated by Mg^{2+} and 1.5 times if Ca^{2+} is used as counter-ion. Instead, the energy of sugar-polymer interactions is almost the same and lower than the interaction energies obtained for the Na^+ complexes, so that it cannot be directly correlated to the counter-ion impact on the sugar flux.

Glucose – water adducts can be extracted from the optimized complexes interacting with the neutralized monomers (see Table 3, $\Delta E_{sugar-water}$). Again one can see that these values do not change significantly as a function of the counter-ions. But, compared to the value obtained for the water cluster–sugar interaction energy in vacuum, −101.5 kcal/mol, computed in Section 3.1 (see Fig. 4), one can observe that the interaction energy between glucose and water is lowered when the glucose is interacting with the neutralized monomer. However, this change does not depend strongly on the type of counter-ion attached to the polymer backbone, since the values obtained with the different cations are comparable.

Looking more closely to the interaction points, one can observe that only the water molecules near the cations and the monomers are affected by their presence. An example is illustrated in Fig. 7, obtained for the complex containing Mg^{2+}. In Fig. 7 (right), representing the initial geometry of the complex, the H-bond between the hydrogen C and the oxygen D, in the glucose hydration shell, is broken while a noncovalent interaction between the hydrogen A of the same molecules and oxygen B of the functional SO_3^- group is formed, as shown in the optimized complex in Fig. 7 (center). Thus, the energy loss passing from the hydrated sugar in vacuum to the hydrated sugar linked to the functional monomers, is probably caused by a rearrangement of the noncovalent interactions of the outer water molecules.

Finally, the energies related to the interactions between sugar and monomers, equilibrated with different cations, are too similar and in opposite direction to explain the variations of the glucose flux versus the membrane counter-ion, as previously measured [9].

3.2.2. *Polymer – polymer interactions*

Once analyzed the interaction between glucose and equilibrated monomers, the hydrated monomers (i.e. hydrated building blocks) were used to build some larger fragments of the polymer chain. For each fragment, 7 monomers of styrene with 3 sulfonic groups, neutralized with Na^+, were used as shown in Fig. 8, meanwhile, 4 functional monomers with Ca^{2+} and Mg^{2+} were used to describe the interactions between the polymer chains containing these bivalent ions as shown in Figs. 9 and 10.

The optimizations of the geometries of single polymer fragment were first carried out following the described conformational analysis. Then, each optimized fragment was used to build a larger system formed by two fragments posted as a mirror image. These structures, shown in the aforementioned Figures, were further used as initial geometries for the successive optimizations and therefore used for the evaluation of the related interaction energies.

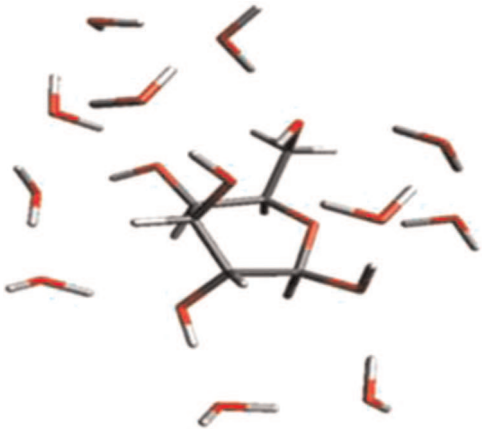

Fig. 4. QM optimized structure of the hydrated glucose in vacuum, i.e. the glucose $(H_2O)_{11}$.

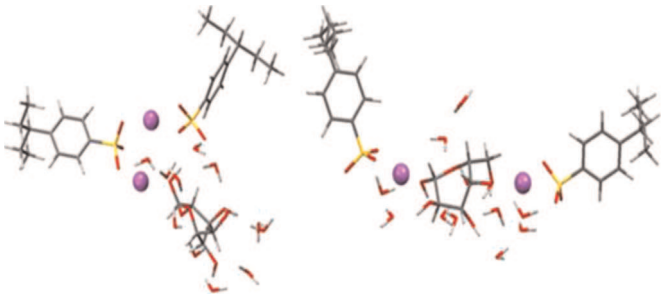

Fig. 5. Equilibrium (optimized) arrangements of 2 functionalized monomers neutralized by 2 Na^+ around the hydrated glucose.

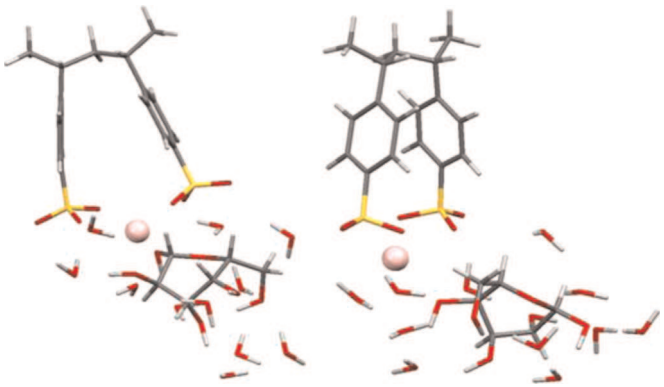

Fig. 6. Equilibrium arrangements of 2 functionalized monomers neutralized by 1 Ca^{2+} around the hydrated glucose.

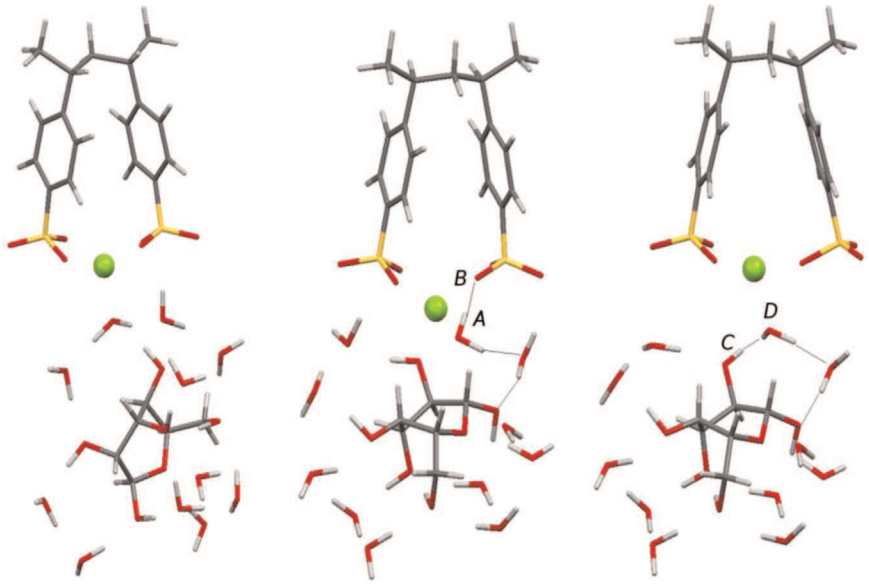

Fig. 7. Equilibrium arrangements of 2 functionalized monomers neutralized by 1 Mg^{2+} around hydrated glucose (left and center). Complex used as starting geometry for the successive QM/MM optimizations (right).

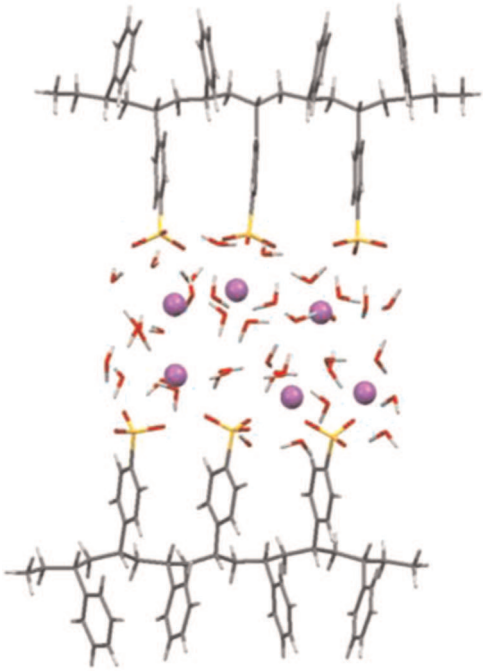

Fig. 8. Optimized geometry of macromolecular model formed by two polymer fragments equilibrated by Na^{+}.

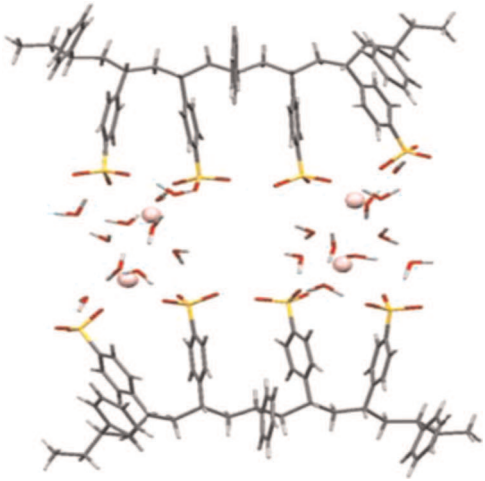

Fig. 9. Optimized geometry of macromolecular model formed by two polymer fragments equilibrated by Ca^{2+}.

A modification of the membrane properties themselves, according to the counter-ion, is another possibility to explain the changes of the sugar flux as observed experimentally. Based on the finding concerning the interactions of the hydrated glucose, the interactions between two fragments of the polymer chain were hence evaluated.

First, the average distances between the cations and the $-SO_3^-$ groups along the same polymer fragment were calculated and reported in Table 4.

Moreover, the average distances between an oxygen atom of a fragment and the nearest oxygen atom of the other were also estimated. Their values are also reported in Table 4. One can observe that the average distance between two neighbor oxygen atoms in two polymer fragments varies according to the nature of cation.

According to Karpenko-Jereb et al. [30], these distances can be linked to the solute transfer in the membrane. More precisely, increasing distance should give higher solute flux. Then, the sugar fluxes obtained during previous experimental investigation [9] are plotted in Fig. 11 versus the computed values of SO^{3-}-cation and chain – chain distances obtained in the present work. One can observe that, for the 3 sugars investigated, the flux increases with the distance in a linear manner.

On the other hand, concerning glucose sizes, the values of the minimum size, $d_{min,}$ at different hydration levels as well as those of the effective diameter, $d_{eff,}$ were computed and reported in Table 2 (Section 3.1). One can state that the values of the chain-chain distance are of the same range of magnitude of the minimum molecular size d_{min} of glucose, ranging from 7.3 up to 8. However, the values of the effective diameter of glucose are much higher (about twice).

The large models used here to compute the distances between the polymer fragments has to be considered as a good approximation of the bottlenecks encountered by the sugar during its transfer through the membrane. Although, longer polymer

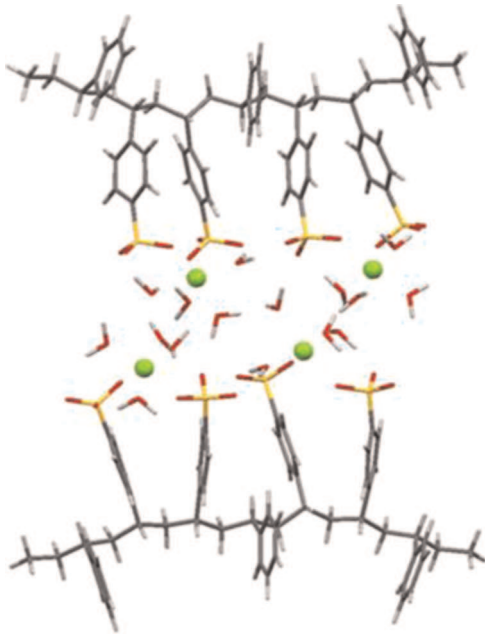

Fig. 10. Optimized geometry of macromolecular model formed by two polymer fragments equilibrated by Mg^{2+}.

Table 4
Average distances between the cations and the $-SO_3^-$ groups for the system optimized in QM/MM.

Cation	Cation-SO_3^- distance (Å)	Chain – chain distance (Å)
Na^+	3.09	8.57
Ca^{2+}	2.42	7.56
Mg^{2+}	2.08	6.46

fragments could be necessary to represent the whole membrane polymer structure and to obtain more accurate average chain – - chain distances, but the interactions considered here work at the nanoscale level thus the used models are large enough to describe such interactions of interest. In addition, by this dimensional comparison, which nevertheless correlates with the experimental trend of the sugar flux, one can suggest that a stretch of the polymer chains, i.e. an increase of the chain – chain average distance, should take place in order to permit the diffusion of the hydrated sugar into the polymer matrix. The change of the sugar flux as function of the counter-ion could be linked more likely to a dynamic change in the chain – chain distance than to the average chain – chain distance in a static equilibrium. In other words, since the noncovalent interactions at nanoscale level can be responsible of the polymer breath, thus of the dynamic chain – chain distances, one can imagine that these interactions could vary according to the cation used as counter-ion, so, the dynamic chain – chain distance may change.

Table 5
Energies, $\Delta E_{frag-frag}$, of the interactions between polymer fragments (evaluated using macromolecular models); number of H_2O molecules and H-Bond wires trapped in the polymer fragments; interaction energies per trapped H_2O molecule and H-Bond wire.

Cation	*$\Delta E_{frag-frag}$ (kcal/mol)*	*N° trapped H_2O*	*N° H-bond wire*	*ΔE^x_{H2O} (kcal/mol)*	*ΔE^x_{Hwire} (kcal/mol)*
Na^+	−200.62	36	7	−5.57	−28.66
Ca^{2+}	−166.70	20	3	−8.33	−55.57
Mg^{2+}	−232.29	16	3	−14.52	−77.43

To check this assumption, the enlargement of the chain – chain distance was considered and specially, it is correlated with the energies associated to the interactions between the polymer chains, $\Delta E^x_{frag-frag}$ which were evaluated using fragments equilibrated with the investigated counter-ions. The values were reported in Table 5 together with those of $\Delta \overline{E}^x_{H_2O}$, which is the interaction energy per water molecule trapped in two polymer fragments for a given counter-ion, *x*, (i.e. Na^+, Ca^{2+} and Mg^{2+}), that can be calculated using the following equation, where (N_{H2O}) is the number of water molecules entrapped between two polymer fragments:

$$\overline{\Delta E}^x_{H_2O} = \frac{\Delta E^x_{frag-frag}}{N_{H_2O}} \quad (1)$$

In other terms, the total cohesion energy between two polymer fragments is distributed among the water molecules embedded between these fragments. Thus, $\overline{\Delta E}^x_{H_2O}$ is the average energy associated to the noncovalent (electrostatic) interactions that each water molecule, belonging to one polymer fragment, exerts on the other hydrated fragment. According to its definition, $\overline{\Delta E}^x_{H_2O}$ does not take into account the interactions between water molecules belonging to the same fragment. Moreover, it is very important to emphasize that the number of water molecules, N_{H2O}, used to

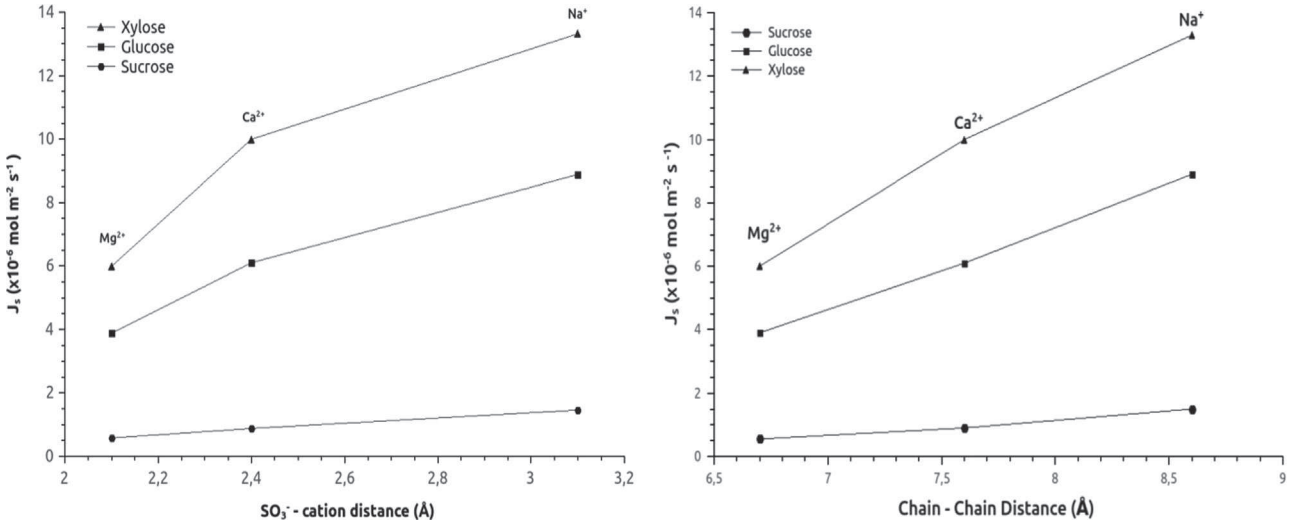

Fig. 11. Experimental fluxes in CMX membrane equilibrated with different counter-ion vs. the counter-ion – SO_3^- distance (left) and chain – chain distance (right).

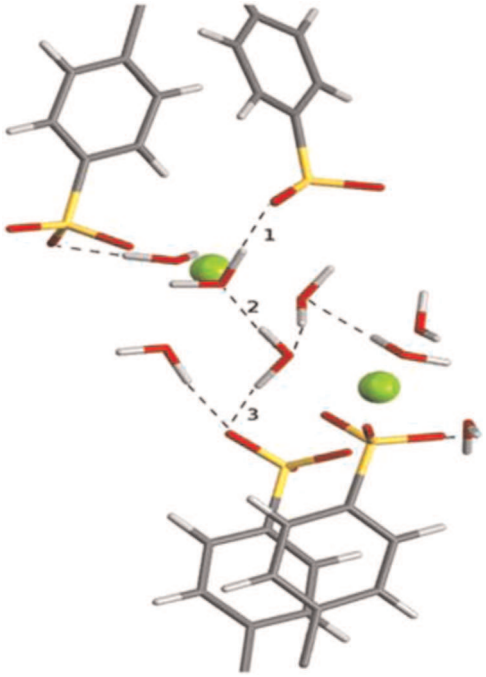

Fig. 12. H-bond path indicated by 1, 2 and 3 and connecting oxygen of the $-SO_3^-$ group with oxygen of sulfonic group located on other chain fragment.

calculate $\overline{\Delta E}^{x}_{H_2O}$ energies by Eq. (1) is not arbitrarily chosen. The value considered is that previously obtained by using a high level of quantum theory reported in Table 1, as described in Section 2, i.e. the computed number of water molecules in the first hydration shell of the investigated counter-ions interacting with the polymer backbone. Not only the number of water molecules but also their arrangements inside the polymer fragments were the result of accurate QM/MM optimizations.

It is worth noting that while $\Delta E^{x}_{frag-frag}$ does not have a direct physical interpretation as the polymer chains are packed one with the other in the membrane, hence it is difficult to extract from the $\Delta E^{x}_{frag-frag}$ real adherence of the chains. On the contrary, $\overline{\Delta E}^{X}_{H_2O}$ has a direct interpretation since it is the average noncovalent interactions of each water molecule bound to the polymer fragments, therefore associated to the mobility of the confined molecules and then to a measurable quantity.

For further analysis on the cohesion energy among polymer fragments, wires or paths (H-bond wire), formed by water molecules linked one to the other by hydrogen bonds, were also identified in the optimized macromolecular models. As shown in Fig. 12, an H-bond wire is defined as the shortest path, i.e. the path with the least number of hydrogen bonds, connecting two oxygen atoms of SO_3^- groups located in two different chain fragments. The dead-end paths, shown Fig.12, were not counted in the total number of wires while the OH bonds with lengths up to 2.1 Å and a cutoff value angle of 120 ° were considered as hydrogen-bonding interactions [27].

As previously for $\overline{\Delta E}^{x}_{H_2O}$, the ratio between the total interaction energy, $\Delta E_{frag-frag}$ and the number of H-bond wires, N_{Hwire}, found in the optimized macromolecular structures, was calculated:

$$\overline{\Delta E}^{x}_{wire} = \frac{\Delta E^{x}_{frag-frag}}{N_{wire}} \quad (2)$$

$\overline{\Delta E}^{x}_{wire}$ is the electrostatic interaction energy per H-bond wire. Here, the total interaction energy between two fragments was distributed only among the water molecular wires (paths) connecting them, not on every trapped water molecules. Thus, this quantity estimates the cohesion energy between two adjacent polymer chains that resist to deformations of the polymeric structure of the membrane. Both values are reported in Table 5.

The contributions taken into account by $\overline{\Delta E}^{x}_{wire}$ are the same as those considered by $\overline{\Delta E}^{x}_{H_2O}$, as well as the physical interpretation. However, the quantities reveal two different behaviors since $\overline{\Delta E}^{x}_{H_2O}$ underlines the crucial role of the water in the supramolecular structure in a wet CMX membrane, while $\overline{\Delta E}^{x}_{wire}$ emphasizes the function of the H-bonds paths as “cohesion bridge” (physical crosslink) between two polymer chains into the membrane polymeric structure. Nevertheless, one can expect that higher values of any of them, revealing stronger interactions *inside* the polymer matrix, should correspond to lower values of the sugar flux.

Fig. 13 shows the variation of the experimental sugar flux *(macroscopic quantity)* versus the absolute value of $\overline{\Delta E}^{X}_{H_2O}$ on one hand and $\overline{\Delta E}^{X}_{wire}$ on the other hand *(nanoscopic quantities)*.

One can observe that for the 3 sugars investigated, the flux decreases with the absolute value of interaction energy. This result is physically consistent since the increase of the cohesion between the water molecules trapped in the two polymer chains or the energy of the cohesion bridge (i.e. physical crosslink) requires a higher energy for the sugar to diffuse through the membrane.

To check further this assumption, the ratios between the

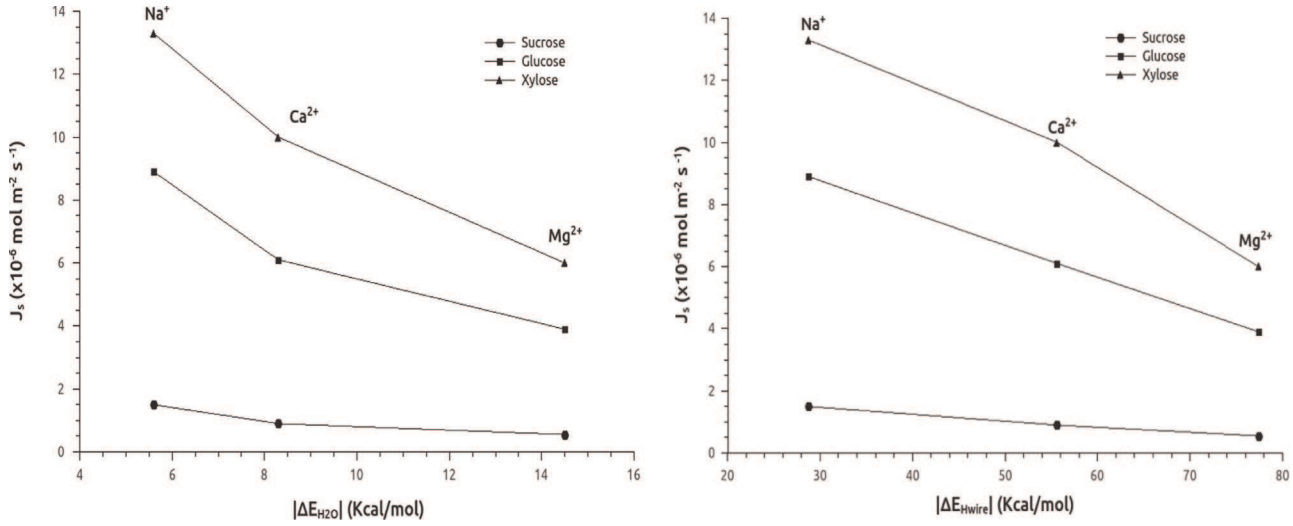

Fig. 13. Variation of sugar flux in function of energies absolute values $\overline{\Delta E}^{X}_{H_2O}$ (left) and $\overline{\Delta E}^{X}_{wire}$ (right) computed in presence of different cations used as counter-ion.

Table 6
Ratios between xylose, glucose and sucrose normalized experimental fluxes and theoretical ratios between the corresponding $\overline{\Delta E}^{X}_{H_2O}$ or $\overline{\Delta E}^{X}_{wire}$ energies.

Cation	$\frac{J_{Na}}{J_x}$(xylose)	$\frac{J_{Na}}{J_x}$(glucose)	$\frac{J_{Na}}{J_x}$(sucrose)	$\frac{\overline{\Delta E}^{X}_{H_2O}}{\overline{\Delta E}^{Na}_{H_2O}}$	$\frac{\overline{\Delta E}^{X}_{wire}}{\overline{\Delta E}^{Na}_{wire}}$
Ca^{2+}	*1.33*	*1.45*	*1.66*	*1.49*	*1.94*
Mg^{2+}	*2.22*	*2.28*	*2.50*	*2.61*	*2.70*

experimental sugar fluxes and the corresponding computed values of $\overline{\Delta E}^{X}_{H_2O}$ and $\overline{\Delta E}^{X}_{wire}$ were evaluated. Furthermore, in order to normalize the values, the system equilibrated with Na^+ is considered as reference and the following equations have to be checked:

$$\frac{J_{Na}}{J_x} = \frac{\overline{\Delta E}^{X}_{H_2O}}{\overline{\Delta E}^{Na}_{H_2O}} \tag{3}$$

and

$$\frac{J_{Na}}{J_x} = \frac{\overline{\Delta E}^{X}_{wire}}{\overline{\Delta E}^{Na}_{wire}} \tag{4}$$

In Table 6, the values of the normalized experimental fluxes of xylose, glucose and sucrose, are reported together with the corresponding theoretical ratios defined in Eqs. (3) and (4). One can observe that, for a given sugar, the theoretical ratios are in the same range as the mean values of the normalized flux, obtained with the two investigated cations.

It means that the polymer fragments cohesion energy *per* embedded water molecules or *per* H-Bond wire is the driving force determining the influence of the counter-ion on the sugar flux. Thus, it can be assumed that the fluxes of organic molecules are driven by the noncovalent interactions carried out via single connecting molecular path or water molecules trapped in the polymer filaments. The intermolecular interactions, governing the transport of the sugar, come from water clusters that by means of hydrogen-bonding interactions form connecting paths between the polymer fragments. In light of this finding, one can clearly emphasize the role of water – cation interactions on the transfer of sugars. These interactions determine the number of water molecules entrapped in the polymer as well as the arrangement of those water molecules between the polymer chains. Although of lesser impact, other mechanisms could also be involved, as indicated by the slight dependence of the normalized flux with respect to the kind of sugar. In particular, the differences between the normalized fluxes can derive from structural diversity of the sugars, such as size or number of OH groups for instance, that can also affect the transfer through the membrane, but probably independently from the counter-ion.

4. Conclusions

In a previous work, the fluxes of sugars in aqueous solutions were measured through a CMX cation exchange membrane, composed by sulfonated polystyrene-divinylbenzene and neutralized with Na^+, Ca^{2+} and Mg^{2+} cations. It was shown that the flux is fixed according to the membrane counter-ion [9]. Higher fluxes were observed when the membrane is equilibrated with a lesser hydrated counter-ion in solution. The purpose of this work was to carry a computational investigation, at the nanoscale level, to determine the main interactions and related mechanism responsible for the change of the sugar transfer according to the membrane counter-ion.

Noncovalent interactions between hydrated glucose and sulfonated styrene monomers as well as interactions between polymer fragments were investigated by using accurate QM and QM/MM approaches. Macromolecular complexes were used to investigate the glucose solubility inside the polymer as well as the chain – chain interactions as function of the nature of counter-ion.

Analyzing the hydration of the investigated counter-ions in sulfonated styrene monomers, it was shown that the number of water molecules in the first hydration shell decreases ($Na^+ > Ca^{2+} > Mg^{2+}$) as the experimental fluxes of the sugars. The hydration of the cations, in the polymer matrix, is the inverse than in solution due to steric hindrance of adjacent -SO_3^- groups along the polymer chain necessary to balance the charge of the divalent ions. The interaction energies between the functional monomers and the hydrated glucose, related to the sugar solubility, were found to be almost independent from the cation. Meanwhile, the negative energy values showed that the sugar can be considered as dissolved in the matrix, while its solubility is not affected by the nature of the cations.

The interactions between polymer fragments were also investigated using macromolecular models. Unlike sugar – fragment interactions, it was found that fragment – fragment interactions are very sensitive to the membrane counter ion.

First, the average distances between the counter-ions and the oxygen of the sulfonic group belonging to the same fragment as well as the distances between two optimized polymer fragments were found to vary with the cation nature. Then, due to the decrease of the fragment – fragment distance, a lower sugar flux can be expected. This is effectively what was observed considering the variations of the experimental values of the sugar flux versus the computed values of the two distances. Moreover, the computed value of the minimum diameter of the hydrated glucose was found to be in the range of those distances. But a comparison of these distances with the computed effective diameter of the hydrated glucose showed that another mechanism should be involved to explain the experimental results.

Then, the fluxes were plotted versus the polymer fragments cohesion energy *per* embedded water molecules or *per* H-Bond wire. It was found that for the 3 sugars investigated, the flux decreases when the aforementioned interaction energies increase. Thus, it seems that, in the conditions investigated, the fluxes of organic molecules are driven by the noncovalent interactions in which single connecting water paths or mobility of the water molecules trapped in the polymer filaments are involved. This work has shown that these noncovalent interactions depend on the nature of the counter-ion. Moreover, it has highlighted the crucial role of the water molecules coordinating the counter-ions in the polymer network. If the aforementioned average distance between one oxygen atom of one fragment and the nearest oxygen of the other seems to be linked to the necessity of a polymer chains enlargement, $\overline{\Delta E}^{x}_{H_2O}$ and $\overline{\Delta E}^{x}_{wire}$ can be correlated to the required energy to make this happen, in the sense that trapped water molecules move to the passage of the sugar. More precisely, it is the energy of temporary break of the connections between the polymer chains, which depends on the membrane counter ion, allowing the solute diffusion through the membrane.In dense membranes like that investigated here the transfer occurs in free volume elements, i.e. those accessible to the solute. It was also suggested that in certain conditions the free volume can vary with the polymer breath, corresponding to the widening and narrowing of the polymeric chains, i.e. the breaking and formation of noncovalent bonds among the trapped water molecules in the polymer network. Then, the solute opens a path in the polymer matrix following the break of the connections between the polymers

chains, these connections being formed again after its passage. From this work, it seems that, in the conditions investigated, such a polymer breath, affected by the membrane counter-ions, is the main mechanism fixing the solute transfer as observed at the macroscopic level. In addition, since the proposed ab-initio interpretation and correlations are carried out without using adjustable or empirical parameters, this represents a significant step forward to the reliability of the predictions.

Acknowledgments

The authors would like to thank The Education, Audiovisual and Culture Executive Agency (EACEA) under the Program "Erasmus Mundus Doctorate in Membrane Engineering" – EUDIME (FPA 2011-0014, http://www.eudime.unical.it) for funding this research. In addition, they are grateful to the support of the Cineca supercomputing center.

References

[1] Global Footprint Network, August 19th is Earth Overshoot Day: The date our Ecological Footprint exceeds our planet's annual budget, 2014.
[2] E. Drioli, E. Curcio, Perspective membrane engineering for process intensification: a perspective, J. Chem. Technol. Biotechnol. 82 (2007) 223–227.
[3] E. Drioli, A.I. Stankiewicz, F. Macedonio, Membrane engineering in process intensification – an overview, J. Membr. Sci. 380 (2011) 1–8.
[4] B. Van der Bruggen, E. Curcio, E. Drioli, Process intensification in the textile industry: the role of membrane technology, J Environ. Manag. (2004) 267–274.
[5] M. Sadrzadeh, T. Mohammadi, Sea water desalination using electrodialysis, Desalination 221 (2008) 440–447.
[6] G.M. Geise, D.R. Paul, B.D. Freeman, Fundamental water and salt transport properties of polymeric materials, Prog. Polym. Sci. 39 (2014) 1–42.
[7] M.A. Shannon, P.W. Bohn, M. Elimelech, J.G. Georgiadis, B.J. Mariñas, A. M. Mayes, Science and technology for water purification in the coming decades, Nature 452 (2008) 301–310.
[8] H. Strathmann, Electrodialysis, a mature technology with a multitude of new applications, Desalination 264 (2010) 268–288.
[9] S. Galier, J. Savignac, H. Roux-de Balmann, Influence of the ionic composition on the diffusion mass transfer of saccharides through a cation-exchange membrane, Sep. Purif. Technol. 109 (2013) 1–8.
[10] G. De Luca, F. Bisignano, A. Figoli, F. Galiano, E. Furia, R. Mancuso, O. Saoncella, M. Carraro, M. Bonchio, B. Gabriele, Bromide ion exchange with a Keggin polyoxometalate on functionalized polymeric membranes: a theoretical and experimental study, J. Phys. Chem. B 118 (2014) 2396–2404.
[11] G. De Luca, L. Donato, S. García Del Blanco, F. Tasselli, E. Drioli, On the cause of controlling affinity to small molecules of imprinted polymeric membranes prepared by noncovalent approach: a computational and experimental investigation, J. Phys. Chem. B 115 (2011) 9345–9351.
[12] G. De Luca, A. Gugliuzza, E. Drioli, Competitive hydrogen-bonding interactions in modified polymer membranes: a density functional theory investigation, J. Phys. Chem. B 113 (2009) 5473–5477.
[13] G. De Luca, F. Bisignano, F. Paone, S. Curcio, Multi-scale modeling of protein fouling in ultrafiltration process, J. Membr. Sci. 452 (2014) 400–414.
[14] V.V. Barkaline, Y.V. Douhaya, A. Tsakalof, Computer simulation based selection of optimal monomer for imprinting of tri-O-acetiladenosine in polymer matrix: vacuum calculations, J. Mol. Model. 19 (2013) 359–369.
[15] V. Busico, R. Cipullo, N. Friederichs, S. Ronca, G. Talarico, M. Togrou, B. Wang, Block copolymers of highly isotactic polypropylene via controlled Ziegler-Natta polymerization, Macromolecules 37 (2004) 8201–8203.
[16] X. Kang, Y. Song, Y. Luo, G. Li, Z. Hou, J. Qu, Computational studies on isospecific polymerization of 1-hexene catalyzed by cationic rare earth metal alkyl complex bearing a C 3 i Pr-trisox ligand, Macromolecules 45 (2012) 640–651.
[17] M.D. Hanwell, D.E. Curtis, D.C. Lonie, T. Vandermeersch, E. Zurek, G. R. Hutchison, Avogadro: an advanced semantic chemical editor, visualization, and analysis platform, J. Cheminform. 4 (2012) 17.
[18] A.K. Rappé, C.J. Casewit, K.S. Colwell, W.A. Goddard III, W.M. Skiff, UFF, a full periodic table force field for molecular mechanics and molecular dynamics simulations, J. Am. Chem. Soc. 114 (1982) 10024–10035.
[19] M. Valiev, E.J. Bylaska, N. Govind, K. Kowalski, T.P. Straatsma, H.J.J. van Dam, D. Wang, J. Nieplocha, E. Apra, T.L. Windus, W.A. de Jong, NWChem: a comprehensive and scalable open-source solution for large scale molecular simulations, Comput. Phys. Commun. 181 (2010) 1477–1489.
[20] T.P. Straatsma, E. Apra, T.L. Windus, M.E. Dupuis, J. Bylaska, W. de Jong, S. Hirata, D.M. Smith, A.M. Hackler, T.L. Pollack, R.J. Harrison, J. Nieplocha, V. Tipparaju, M. Krishnan, E. Brown, G. Cisneros, G.I. Fann, H. Fruchtl, J. Garza, K. Hirao, R. Kendall, J.A. Nichols, K. Tsemekhman, M. Valiev, K. Wolinski, J. Anchell, D. Bernholdt, P. Borowski, T. Clark, D. Clerc, H. Dachsel, M. Deegan, K. Dyall, D. Elwood, E. Glendening, M. Gutowski, A. Hess, J. Jaffe, B. Johnson, J. Ju, R. Kobayashi, R. Kutteh, Z. Lin, R. Littlefield, X. Long, B. Meng, T. Nakajima, S. Niu, M. Rosing, G. Sandrone, M. Stave, H. Taylor, G. Thomas, J. van Lenthe, A. Wong, Z. Zhang, NWChem, A Computational Chemistry Package for Parallel Computers, version 6.1.1, Pacific Northwest National Laboratory, Richland, WA, 2005.
[21] X. Xu, Q. Zhang, R.P. Muller, W.A. Goddard III, An extended hybrid density functional (X3LYP) with improved descriptions of nonbond interactions and thermodynamic properties of molecular systems, J. Chem. Phys 122 (2005) 014105.
[22] S. Simon, M. Duran, J.J. Dannenberg, How does basis set superposition error change the potential surfaces for hydrogen-bonded dimers? J. Chem. Phys. 105 (1996) 11024.
[23] W.D. Cornell, P. Cieplak, C.I. Bayly, I.R. Gould, K.M. Merz, D.M. Ferguson, D. C. Spellmeyer, T. Fox, J.W. Caldwell, P.A. Kollman, A second generation force field for the simulation of proteins, nucleic acids, and organic molecules, J. Am. Chem. Soc. 117 (1995) 5179–5197.
[24] C.L. Brooks III, A.D. Mackerell, L. Nilsson, R.J. Petrella, B. Roux, Y. Won, G. Archontis, C. Bartels, S. Boresch, A. Caflisch, L. Caves, Q. Cui, A.R. Dinner, M. Feig, S. Fischer, J. Gao, M. Hodoscek, W. Im, K. Kuczera, T. Lazaridis, V. Ovchinnikov, E. Paci, R.W. Pastor, C.B. Post, J.Z. Pu, M. Schaefer, B. Tidor, R. M. Venable, H.L. Woodcock, X. Wu, W. Yang, D.M. York, M. Karplus, N. Heart, A. Arbor, J. Comput. Chem., 30, (2009) 1545.
[25] D. Beglov, B. Roux, Finite representation of an infinite bulk system: solvent boundary potential for computer simulations, J. Chem. Phys. 100 (1994) 9050.
[26] A. Fuoco, Computational and Experimental Studies on Membrane – solute Interactions in Desalination Systems Using Ionic-exchange Membrane, Ph.D. Thesis Universitè Paul Sabatier, Toulouse, France, 2015.
[27] S.J. Grabowski, W.A. Sokalski, E. Dyguda, J. Leszczyn, Quantitative classification of covalent and noncovalent H-bonds, J. Phys. Chem. B 110 (2006) 6444–6446.
[28] A. Buekenhoudt, F. Bisignano, G. De Luca, P. Vandezande, M. Wouters, K. Verhulst, Unravelling the solvent flux behaviour of ceramic nanofiltration and ultrafiltration membranes, J. Membr. Sci. 439 (2013) 36–47.
[29] F. Bisignano, Modeling of nanostructured membranes for wastewater purification, Dottorato in Scienza e Tecnica Bernardino Telesio Curriculum M3, XXVI ciclo, Università della Calabria, Italy, 2014.
[30] L.V. Karpenko-Jereb, A.-M. Kelterer, N.P. Berezina, A.V. Pimenov, Conductometric and computational study of cationic polymer membranes in H+ and Na+-forms at various hydration levels, J. Membr. Sci. 444 (2013) 127–138.